Sādhanā (2020)45:232
https://doi.org/10.1007/s12046-020-01436-9

A novel image compression model by adaptive vector quantization: modified rider optimization algorithm

PRATIBHA PRAMOD CHAVAN[1,2], B SHEELA RANI[1,*], M MURUGAN[3] and PRAMOD CHAVAN[4]

[1]Sathyabama Institute of Science and Technology (Deemed to be University), Jeppiaar Nagar, Rajiv Gandhi Salai, Chennai 600 119, Tamil Nadu, India
[2]Department of E&TC Engineering, Trinity College of Engineering and Research, Pisoli, Pune 411 048, Maharashtra, India
[3]ECE Department, SRM Valliammai Engineering College, Kattankulathur, Chengalpet (Dist.) 603 203, Tamil Nadu, India
[4]Department of E&TC Engineering, K J College of Engineering and Management Research, Pisoli, Pune 411048, Maharashtra, India
e-mail: cpratibhapramod@gmail.com; sheelarani@sathyabama.ac.in; dr.murugan.m@gmail.com; pramodp.chavan@gmail.com

MS received 17 September 2019; revised 9 May 2020; accepted 15 May 2020

Abstract. In recent days over the internet, the uploading of enormous new images is being made every day, and they necessitate large storage to accumulate the image data. For the earlier few decades, more analysts have evolved skillful image compression schemes to enhance the compression rates and the image quality. In this work, Vector Quantization is used, which uses the *Linde–Buzo–Gray algorithm*. As a novel intention, the codebooks are optimized by an improved optimization algorithm. In this approach, the database image is firstly separated into a set of blocks, i.e., pixels, and these sets of blocks are referred to as vectors. Then a suitable codeword is selected for each vector such that is the closest representation of that input vector. The encoder generates a codebook by mapping the vectors on the basis of these code words, and the compression of the vectors takes place. The encoder then sends a compressed stream of these vectors by pointing out their indices from the codebook to the decoder through a channel. The decoder then decodes the index to find out the compressed vector and places it on the image. For attaining a better image compression effect, the codebook is optimized using the Best Fitness Updated Rider Optimization Algorithm. The optimization of codebooks is done so that the summation of the compression ratio and the error difference between the original and decompressed images has to be minimized. Moreover, the proposed model is scruntized with other existing algorithms, and the experimental outcomes are validated.

Keywords. Image compression; vector quantization; Linde–Buzo–Gray; codebook; rider optimization algorithm; fitness.

1. Introduction

Image compression [1–3] is considered as the progression of minimizing the byte size in a graphics file in spite of weakening the quality of image to a detrimental level. The file size minimization thus authorizes more images to be accumulated around the disk or memory space in specified amount. The time needed for the transmission of image around the Internet or downloaded from Web pages is as well minimized [4–6]. Various novel approaches are in the literature for the image files to be compressed. Typically, more used image formats for the compressed graphic in the internet are GIF format and the JPEG format. We all know that the JPEG model and GIF images are commonly facilitated for images and, line art erstwhile images, respectively, wherein the geometric shapes are fairly easier [7–10].

The typical categorization of image compression techniques are mainly of two types, (a) Lossy Compression and (b) Lossless Compression. The compression of text file or program can be made to a particular extent only and is exploited as lossless compression. On exceeding this threshold, errors may occur [11]. The redundancy is used by the Lossless image compression

*For correspondence
Published online: 09 September 2020

techniques with no loss of data [12, 13]. As a result, there seems a close similarity among the data stream earlier to encoding and successive to decoding, and has not noted any deformation in the restoration quality. Both the lossy and lossless compressions are two diverse processes, which are reversible to one another [14, 15]. Different from lossless image compression, in restoration phase, the lossy image compression models experience quality loss because of its data loss. Comparatively, the distortion of image into series of symbols is initially exploited in lossy image compression, wherein quantized to a discrete sequence of acceptable levels [16–18].

The other methods for image compression [19–21] consist of the wavelets and fractals schemes. These techniques have not attained extensive application on the Internet. On the other hand, both schemes proffer assurance, since they present a higher compression ratio when compared with the GIF or JPEG models for certain kinds of images. An additional novel technique, which replaces the GIF format, is the PNG format. Firefly algorithm had been utilized for all types of noisy image [22, 23]. In program and text files, it is essential that compression [24–26] be lossless as a particular error can critically break the denotation of a text file, or make a program not to run. For this cause, graphic images could be compressed more than programs or text files [27, 28].

The major contribution of this research work is elucidated as follows.

1. This work exploits the Vector Quantization (VQ) concept that uses the Linde–Buzo–Gray (LBG) model for image compression.
2. Here, the database image is initially split into a set of blocks. Subsequently, an appropriate code word is chosen for every vector, which is the closest representation of that input vector.
3. For an improved image compression effect, the code word generation in LBG-based VQ is optimized by the proposed Best Fitness Updated Rider Optimization Algorithm (BFU-ROA) model.
4. The optimization of codebooks should be done so that the summation of the compression ratio and the difference among the decompressed and original images should be minimal.
5. To the end, the implemented BFU-ROA model regarding performance is compared with other classical models, and its enhancement is confirmed through the valuable performance analysis.

The paper is organized as follows. Section 2 analyzes the literature works done on the contributed papers. Section 3 describes the LBG-based vector quantization for image compression and section 4 portrays the initial codebook optimization by proposed BFU-ROA. In addition, section 5 presents the outcomes with discussions and in section 6 the conclusions are provided. .

2. Literature review

2.1 *Related works*

In 2019, Pang *et al* [1] have investigated the QDCT, which was much proficient than its traditional counterparts with respect to intricacy. In addition, the adopted QDCT was exploited to build up and recognize a quantum image compression method. The introduced compression model carries out a search to find out the most considerable evaluated DCT coefficients, which was attained from Grover's approach. Therefore, the introduced model could compute the DCT coefficients concurrently by deploying two predictions. The assessment of the adopted scheme moreover indicates that the implemented scheme was better over the other classical models. Thus, the efficiency of the proposed approach over traditional schemes has been validated.

In 2017, Ferda *et al* [2] have established an approach based on the "*Tchebichef psychovisual*" threshold in order to produce the best image waveform's bits-budget. In image compression, this bits-budget was modeled to restore the major part of quantization tables. The investigation outcomes demonstrated that the established model can develop the visual features of image outcome in a better way. The visual image quality generates reduced artifact impacts and deformation of pixels in the image. Accordingly, a group of bits-budgets offers outstanding development in the quality of the image with reduced bit lengths. Finally, the adopted approach was assessed and promising investigational results were attained when distinguished with the traditional structures.

In 2018, Swalpa *et al* [3] have presented a new approach for computing the affine constraints of fractal encoding to minimize its computational complication. An uncomplicated but proficient estimation of the scaling constraint was obtained that gratifies the entire features essential to attain convergence. It permits to replace the costly procedure with an uncomplicated distribution of two integers. Furthermore, a customized HV block partition system was adopted, and several novel paths to develop the encoding period and decoded superiority, over their traditional models. From the analytical outcomes, it was confirmed that the adopted technique attains better performance identical to the traditional fractal dependent image compression models, in a reduced duration.

In 2017, Tahar *et al* [4] have exploited an enhanced EZW model for attaining a better compression performance with respect to bit rate and PSNR for lossless and lossy image compression, correspondingly. For minimizing the count scanning and symbol duplicates of the prevailing EZW; the adopted system exploits a novel noteworthy symbol map that was symbolized in a more proficient manner. In addition, the adoptedmodel was developed for attaining a scalable image coding by deploying the interdependency of color planes efficiently. Finally, simulation results reveal a

noteworthy performance of the adopted scheme over the traditional EZW and other enhanced models in terms of both subjective and objective principles for various compression schemes.

In 2016, Bin *et al* [5] have implemented DTT and MF theory, and then the N×N DTT matrix was factorized into N+1 SERMs with least rounding errors. Regarding the reality, for proficient lossless image compression, a narrative technique known as iDTT was established to accomplish integer to integer mapping. In addition, a sequence of experimentations was performed, and the outcomes demonstrated that the implemented iDTT scheme not only includes a superior compression rate than iDCT system, however it was well-suited with the extensively deployed JPEG standard.

In 2017, Turcza and Mariusz [6] had introduced a novel near-lossless scheme in WCE for proficient energy image compression. The modeled compressor functions on data directly from the CMOS image sensor with the Bayer CFA. On deploying the established methodology, the exploited compressor attains reduced BER and advanced quality of the image when distinguished with more conventional models. On considering the characteristic WCE images, the compression rate was 3.9, whereas the PSNR was 46.5 dB that reminds increased image quality was attained. Finally, it was illustrated that the presented system increases the overall exactness of the adopted scheme on varied data sets.

In 2015, Zhiyong *et al* [7] have adopted a technique that relies on ROI for improving the compression rate. The image was firstly separated as two regions as (i) ROI and (ii) non-ROI. The designated portions of ROI was then employed with Lossless compression approaches, comprehensively, the erstwhile regions of the image was facilitated with other algorithms. At last, the modeling of group of experimentations was exploited for computing the adopted compression technique's efficacy. Accordingly, the experimental outcomes demonstrated that the adopted system has providedsuperior outcomes than other existing approaches.

In 2016, Chaurasia and Vaishali [8] have established fast fractal compression methodologies depending on feature extraction and pioneering approach for image evaluation. In the adopted model, the complication of the appropriate domain search was minimized by converting the issue to the vector domain from the image domain. Moreover, the developed methodology was examined, which in turn confirmed its efficiency when evaluated with conventional schemes.

(a) Meta-heuristicsbased compression algorithms

In 2018, Karri Chiranjeevi and Uma Ranjan Jena [29] developed CS meta-heuristic optimization approach which optimizes the LBG codebook using the levy flight distribution function that follows the Mantegna's algorithm rather than the Gaussian distribution.

In 2017, Kumar *et al* [30] worked on the effectiveness of the VQ, which relies on the suitable codebook. In this work, they tried hadhybrid approach for the LBG with BAT optimization approach that creates a suitable codebook. The optimization algorithm was used not only for design of codebook but also for the selection of the codebook size.

In 2018, Fonseca *et al* [31], developed a novel VQ codebook design approach based on swarm clustering. This approach was on the basis of the FSS algorithm. The FSS was embedded in LBG approach as a swarm clustering algorithmnamed FSS-LBG.

In 2019, Santosh Kumar and Venkata Ramanaiah [32] developed a novel image compression method exploiting hybrid Jaya–Lion mathematical algorithm that was processed in several sequences of progressions. Here, the image segmentation was handled using the Adaptive ACM that separates or segments the image into two regions such as ROI and non-ROI.

In 2020, Mohamed El-Tokhy [33] worked on the OCR of neutron and X-ray radiography images with least decomposition distortion. Here, ABC and firefly optimal methods were exploited in conjunction with the developed image encoding/decoding as well as decomposition/decompression approaches.

In 2019, Abdulrahman Alturki and Abdulrahman Alrobaian [34], introduced Firefly optimization methodon the basis of the DCT to decide the optimal fitness value for all DCT block. While the fitness values werecalculated for DCT blocks, compression process took place.

2.2 *Motivation*

Table 1 shows the merits and demerits of methodologies used in conventional approaches based on the image compression models. At first, the QDCT algorithm was developed in [1], which offers is proficient, and it computes the DCT coefficients concurrently. However, it needs contemplation on varying degrees. Tchebichef psychovisual algorithm was facilitated in [2] that offers excellent bits-budget and minimizes the artifact impacts, but it is challenged to produce optimal outcomes. In addition, the HV Block partition system approach was elucidated in [3] that offered reduced duration, and it offers the uncomplicated distribution of two integers. However, it has to focus more on fractal coding. Likewise, the EZW scheme was exploited in [4], which offers a reduced bit rate, and it also offers enhanced PSNR, the filter bank has to be chosen more carefully. Also, MF theory was employed in [5], which offers a superior compression rate, and it also provides proficient lossless image compression; however, it is complex due to the requirement of lookup tables.WCE algorithm was explicated in [6] that offered enhanced compression rate and improved PSNR, yet, it includes manufacturing and designing complexities. ROI was

Table 1. Merits and demerits of image compression models using diverse techniques.

Author [citation]	Adopted methodology	Features	Challenges
Chao *et al* [1]	QDCT	•Much proficient •Compute the DCT coefficients concurrently	•Needs contemplation on varying degrees.
Ferda *et al* [2]	Tchebichef psychovisual	•Excellent bits-budget •Reduced artifact impacts	•Challenge to produce optimal outcomes
Swalpa *et al* [3]	HV Block partition system	•Reduced duration •Uncomplicated distribution of two integers	•Have to focus more on fractal coding
Tahar *et al* [4]	EZW model	•Reduced bit rate •Better PSNR	•Filter bank has to be chosen more carefully.
Bin *et al* [5]	MF theory	•Superior compression rate •Proficient lossless image compression	•Complex due to the requirement of lookup tables
Turcza and Mariusz [6]	WCE	•Enhanced compression rate •Improved PSNR	•Manufacturing and designing complexities.
Zhiyong *et al* [7]	ROI	•Better efficiency •The high degree of compression	•Requires contemplation on real-time applications
Chaurasia and Vaishali [8]	FIC model	•Domain search was minimized •Reduced complexity	•High spatial resolution.

implemented in [7], which offers improved efficiency, and as well as gives a large degree of compression rate, but this approach requires deliberation on real-time applications. Moreover, the FIC models algorithm was suggested in [8] that provide reduced complexity, and the domain search was minimized. However, it includes more spatial resolution. Hence, these challenges are need to be taken in the future works for enhancing the image compression models regarding effective performance in the present work.

3. LBG-based vector quantization for image compression

3.1 *Vector quantization*

Effective lossless and lossy compressions schemes can be attained by forming a single block (Grouping and encoding outputs of source). The blocks are viewed as vectors, and thus, it can be termed as "VQ" and it is a fixed to a fixed-length method based on the principle of Block Coding". LBG has adopted a VQ modelling approach depending on a training model. The exploitation of the training sequence avoids the necessity for multidimensional integration, which is regarded as a major issue in modelling of VQ [1, 3]. Every VQ code word indicates a particular sample of source output. On considering input samples of longer sequences, it is feasible to take out the configuration in the source code output. Encoding sequences of samples offers a more proficient code even if the input is arbitrary. It is more beneficial in the lossy compression model as well. "Beneficial" addresses the lower rate of distortion and "rate" indicates the average count of bits for each input sample, and distortion measures may usually be the SNR and MSE. The concept that output encoding sequences could offer a benefit over the encoding of individual samples was confirmed by considering longer input sequences. This addresses that a VQ approach, which works with blocks or sequences of output, would offer certain performance developments.

VQ is performed in 3 phases- (a) encoder, (b) channel and (c) decoder, whose diagrammatic demonstration is revealed in figure 1. It comprises of three blocks, where, everyone includes a varied working model. Encoder section denotes "block 1" that comprises of image vectors production, indexing, and codebook production. Image vectors are produced by partitioning the input image into non-overlapping and instant blocks. Production of a proficient codebook remains the most important task in VQ. It involves a set of code words, whose size is equivalent to the size of the non-overlapping block. A scheme is considered a better one if its produced codebook is proficient. Following the successful production of the codebook, every vector will be indexed with an index number taken from the index table. These numbers are conveyed to the receiver. The indexed numbers are conveyed to the receiver through "block 2". The decoder section includes "block 3" that has reconstructed the image, codebook, and index table. With the help of the receiver index table, the attained indexed numbers are decoded. The codebook at the transmitter and receiver is almost the same. The received index numbers are allocated to its respective code words and they are arranged such that, the size of the input image is similar to that of the reconstructed image.

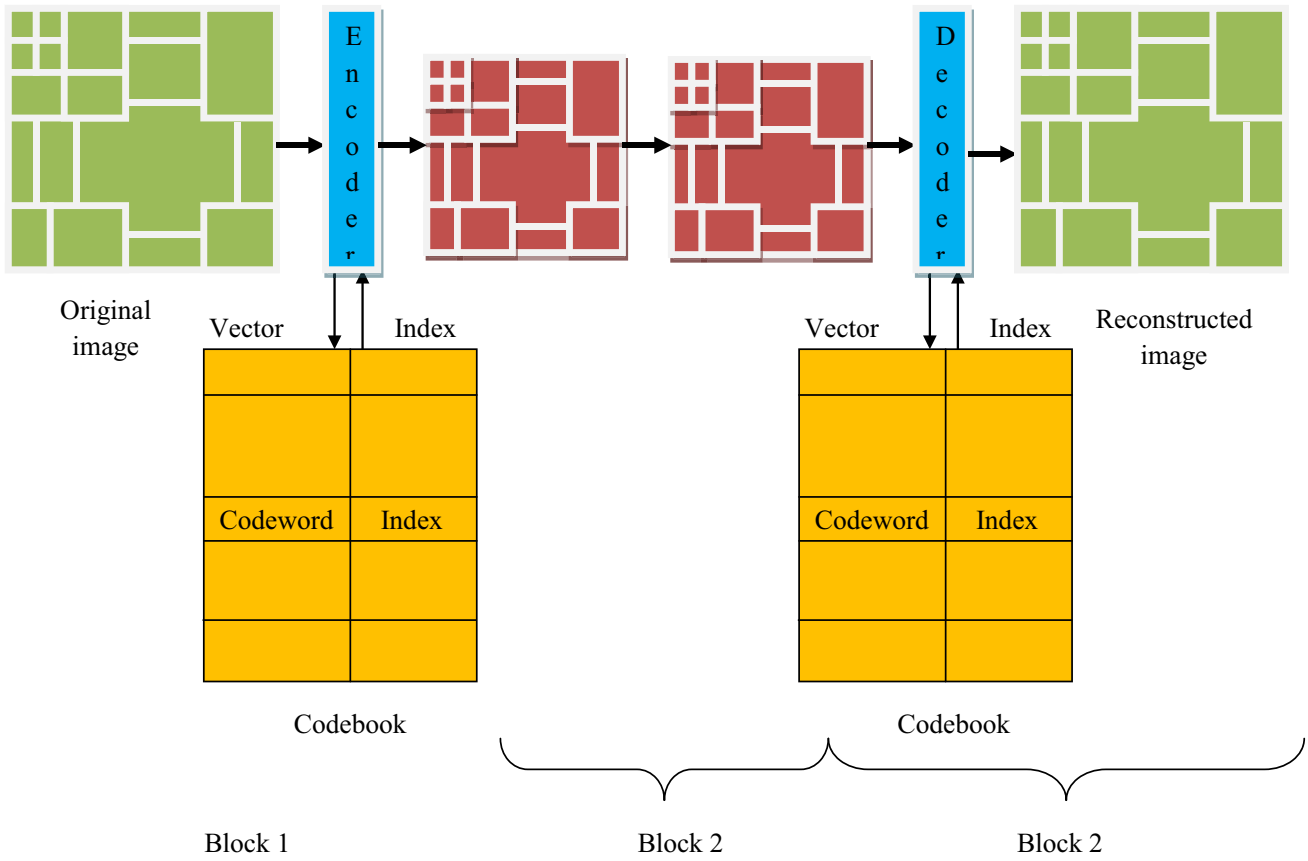

Figure 1. Process of encoding and decoding in Vector Quantization.

3.2 *LBG algorithm*

The LBG approach is an iterative model that necessitates an initial codebook, to begin with. Here, the generation of the codebook is done by means of a training set of images [5], where the set indicates the different kinds of images, which has to be compressed. This codebook (initial) is attained by the "*splitting method*" in the LBG model. In this technique, an initial code vector is fixed as a mean of all the training sequences and is then divided into two. The iterative model is run with the two vectors as an initial codebook, and the last two code vectors are divided into 4, and the procedure is continued till the required count of code vectors is attained [1]. The compression model could be analyzed by specific performances namely, compression rate, PSNR [2].

The group of points at quantizer output is termed as codebook of the quantizer and the procedure of locating these output points is known as "codebook design".

LBG technique is portrayed in the following steps.

1. Begin with an initial set of reconstruction values $\left\{R_i^{(o)}\right\}_{i=1}^{W}$. Assign iteration$p = 0, H^{(o)} = 0$. Choose a threshold$\in$.
2. Discover areas of quantization as per Eq. (1).

$$V_i^{(p)} = \left\{U : h(U, R_i) < h\left(U, R_j\right) \forall j \neq i\right\}\ j = 1, 2..M \tag{1}$$

3. Evaluate distortion as per Eq. (2).

$$H^{(p)} = \sum_{i=1}^{W} \int_{V_i^{(p)}} \left\| U - R_i^{(p)} \right\|^2 fx(U) dU \tag{2}$$

4. If$\frac{\left(H^{(p)} - H^{(p-1)}\right)}{H^{(p)}} < \in$, terminate or continue.
5. $p = p + 1$. Discover novel construction values$\left\{R_i^{(p)}\right\}_{i=1}^{W}$, which are the centroids of$\left\{V_i^{(p-1)}\right\}$. Continue step 2.

This scheme forms the root of the majority of VQ models. It is commonly identified as the LBG approach. The initial codebook for a two level VQ could be attained by incorporating the output point for one level quantizer and a 2^{nd} output point is attained by summing up a predetermined perturbation vector. Further, the LBG model was deployed to attain the two levels VQ. The two codebook vectors are exploited to attain the initial codebook for a 4 level VQ when the algorithm converges. This initial 4

level codebook comprises two codebook vectors from the last codebook of two levels VQ and the other two vectors are attained by summing up to the two codebook vectors. The LBG model was deployed till this 4 level VQ converges. Like this, the levels are doubled till the optimal count of levels is reached. The approach is sustained until the distortion goes below a certain small threshold.

The size of the codebook is raised exponentially with the rate of VQ, which in turn increases the quality of reconstruction; however, the encoding time rises owing to the rise in the computations necessary to discover the nearby matches. On incorporating the last codebook of the preceding phase at each division, it could be assured that the codebook after dividing will be good as the codebook previous to dividing.

4. Initial codebook optimization by the proposed BFU-ROA

4.1 *Codebook optimization*

In the conventional image compression model, the codebooks are generated randomly, however, in the proposed scheme; the codebooks are generated optimally by exploiting an enhanced optimization model called BFU-ROA. Thus, an optimal codebook can be generated as indicated by figure 2, wherein, n indicates the count of generated codebooks.

4.2 *Objective model*

The objective model of the proposed BFU-ROA-based VQ for image compression is to minimize the compression rate and accordingly, the error difference between the decompressed image and original image has to be minimized as shown by Eq. (3). In Eq. (3), E indicates error difference amongst the decompressed and original images, and CI denotes the compression ratio.

$$Min = E + CI \tag{3}$$

$$CI = \frac{Size\ of\ Compressed\ image}{Size\ of\ original\ image} \tag{4}$$

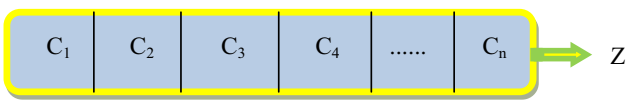

Figure 2. Codebook Encoding.

4.3 *Rider optimization algorithm*

The conventional ROA [35] is the fictional computing optimization algorithm via imaginary concepts and facts. Typically, ROA is dependent on four set of Riders, moving over an identical target to win the chase. The amazing idea concerning ROA is about the improved ROA performance with reduced optimization time, thus performing better than the other artificial computing and meta-heuristic optimizations.

Initialization: The rider's place is initiated as given by Eq. (5), wherein, $Z^{\tau}(g, h)$explicates the location of p^{th} rider atτ. The count of total co-ordinates and riders are expressed as$Y$and$X$. The bypass, followers, over takers, and attackers riders are stated as$B$, F, G and A as per this model.

$$Z^{\tau} = \{Z^{\tau}(g, h)\}; \quad (1 \le g \le X); \quad (1 \le h \le Y) \tag{5}$$

Let the angle related to the vehicle's position, steering, and coordinate of the g^{th} rider is assumed as θ_g, $N^{\tau}_{g,h}$ and δ. In addition, the vehicle coordinates, namely, brake, gear, and accelerator of g^{th} rider are represented as r_g, Q_g and $a_g$in that order. The value of gear Q_g gains amongst 0 and 4, but the brake values r_g and accelerator a_g intercept among 0 and 1.

Computing the success rate: The updating is made for the rider's success rate, so that rider having maximum achievement is announced as the primary or superior rider, relies on whose another rider update oneself. The technique is distanced from local convergence that may be the attacker effect and on the other hand, the overtaker takes the responsibility of global convergence. At first, for reaching the target, the riders go through the efficient random initialization. Besides, the multidirectional search space is formulated by the follower among the leader. Similarly, the success rate is exploited by the overtaker and picks on the optimal dimensional space regarding a directional indicator that attires the optimization at the point of terminal convergence.

Update the leading rider position: The announcing of leading rider is exploited as per the rider's success rate, and the one who leads takes on the position of leader. The rider that closely nearer to the destination is the leader and the leader rider location is the changing sequence that relies on the time. Owing to this, the whole rider's success rate is evaluated and at the iteration end, the leading rider is announced.

Model of the riders' position: Riders are of four stages: bypass rider evades the top path for getting the designation, the leader's path is followed by follower, overtaker takes on the individual path for getting the designation, and attacker sustains the leading rider's position. a predefined policy was chased by every rider for reaching the designation and is made by efficacy managing of brake, accelerator, gear and steering of the vehicle. Regarding these constraints, the position of rider that chases the predefined policy is altered

and this process goes on till τ_{off}off-time. The update of bypass rider is facilitated as in Eq. (6).

$$Z_{g,h}^{\tau+1}(B) = \beta\left[Z_{\gamma,h}^{\tau} * \alpha(h) + Z_{\eta,h}^{\tau} * (1-\alpha(h))\right] \quad (6)$$

In Eq. (6), an number that arbitrarily falls amongst 0 and 1 is stated as β, ηexplicates the number that arbitrarily lies amongst 1 and X, and γdenotes the number that arbitrarily acquiring the values between 1 and X. Concurrently, χ declares the number that arbitrarily having the range 0 and 1 of $(1 \times Y)$ size. As a result, the rider's updating location is made at the individual's iteration break for ensuring the winner. Additionally, the update of follower's location is done as per the winner for reaching the designation and that is expressed by Eq. (7). Herein, leaders' position be Z^L, b denotes the coordinate selector, $N_{g,b}^{\tau}$elucidates the g^{th} rider's steering angle in b^{th} coordinate, L explicates the index of leader, $Z^L(L, b)$, and $\eth_g^{\tau}$evaluates the distance enclosed by g^{th} rider.

$$Z_{g,h}^{\tau+1}(F) = Z^L(L, b) + \left[\cos\left(N_{g,b}^{\tau}\right) * Z^L(L, b) * \eth_g^{\tau}\right] \quad (7)$$

In [35], the rider enclosed a distance which is computed by multiplying velocity and τ_{off} and is evaluated in Eq. (8).

$$\eth_g^{\tau} = v_g^{\tau} * \left(1/\tau_{off}\right) \quad (8)$$

Regarding the coordinate selector, success rate and direction indicator, the over taker's position with respective update is made as per Eq. (9). Herein, I_g^{τ} demonstrates the g^{th} rider's directional indicator inτ and $Z_{g,b}^{\tau}$ represents the g^{th} rider's position in b^{th} coordinate. Eq. (10) is measured as the consequence of success rate.

$$Z_{g,b}^{\tau+1}(O) = Z_{g,b}^{\tau} + \left[I_g^{\tau} * Z^L(L, b)\right] \quad (9)$$

$$I_g^{\tau} = \left[\frac{2}{1 - \log\left(F_g\right)}\right] - 1 \quad (10)$$

In Eq. (9), F_g explains the g^{th} rider's success rate at τ and amongst X riders, the greater success rate is reported, in which the value falls under the interval 0 and 1. The coordinate selector evaluation is dependent on the locations variation of leading rider and g^{th} rider. Otherwise, the intension of attacker is to arrive at the designation chasing the leader with the identical position update of follower. The attacker's location is evaluated by Eq. (11).

$$Z_{g,h}^{\tau+1}(A) = Z^L(L, b) + \left[\cos\left(N_{g,b}^{\tau}\right) * Z^L(L, b) + \eth_g^{\tau}\right] \quad (11)$$

Re-evaluate the success rate: According to the individual rider's success rate, the locations of rider get updated and the rider is updated as leading one in accordance to their higher success rate.

Update the position of rider constraints at the close: At the iteration end, the update of rider constraints is made and thus the desired solution is determined. As a result, the constraints that needs to be updated comprises the ride off-time, accelerator, steering angle, brake and gear along with the activity counter, and at the iteration end, these constraints get updated.

Termination: The optimization phases are iterated till the close, within which the leading rider could be discovered. The pseudo-code of the existing ROA scheme is portrayed in Algorithm 1.

Algorithm 1: TraditionalRider Optimization Algorithm [35]

Input: rider's arbitrary positions, $Z_{g,b}^{\tau}$

Output: Leading rider, Z^L

Dispense the population

Dispense the constraints of rider

Evaluate the success rate

While, $\tau < \tau_{off}$

for $g = 1$ to X

Update bypass rider'slocationas per Eq. (6)

Update follower'slocation as per Eq. (7)

Update the over taker'slocation as per Eq. (9)

Update attacker'slocation as per Eq. (11)

Grade the riders regardingthe success rate

Picks on the rider with a larger success rate as leader.

Update the rider constraints

Return Z^L

$\tau = \tau + 1$

end for

end while

End

4.4 *Proposed BFU-ROA algorithm*

In the conventional ROA method, the bypass rider positions, follower position, overtaker position and attacker position are updated without finding the best solutions, however, in the implemented approach, the fitness of all solutions are computed and the best fitness solutions are determined. Accordingly, the positions of B, F, G and A are updated based on the first best, the second best, third-best, and fourth-best solutions, respectively. As the entire solutions are updated based on fitness, the adopted technique is

explicated as the BFU-ROAmodel. The pseudo-code of the implemented BFU-ROA scheme is highlighted in Algorithm 2, and the corresponding flowchart is given in figure 3.

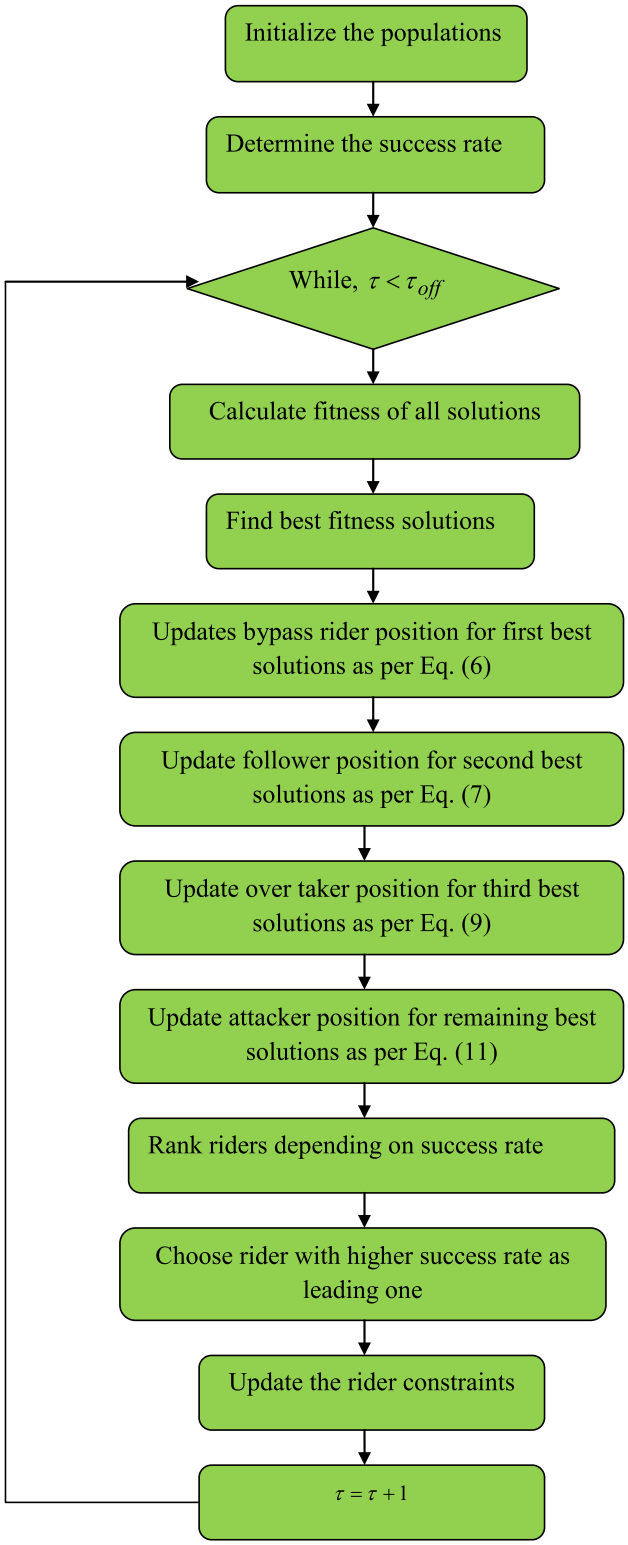

Figure 3. Flow chart of the proposed BFU-ROA model.

Algorithm 2: Proposed BFU-ROA

Input: Random positions of riders, $Z_{g,b}^{\tau}$

Output: Leading rider, Z^{L}

Dispense the population
Dispense the constraints of rider
Evaluate the success rate
While, $\tau < \tau_{off}$
for $g = 1$ to X
Calculate fitness of all solutions
Find best fitness solutions
Update bypass rider location for first best solutions using Eq. (6)
Update follower location for second best solutions using Eq. (7)
Update over taker location for third best solutions using Eq. (9)
Update attacker location for remaining best solutions using Eq. (11)
Grade the riders regarding the success rate
Picks on the rider with a larger success rate as leader.
Update the rider constraints
Return Z^{L}
$\tau = \tau + 1$
end for
end while
End

5. Results and discussions

5.1 *Simulation procedure*

The adopted BFU-ROA-based VQ for image compression was experimented in MATLAB, and the respective outcomes were obtained. In this experimental study, the database considered for image compression consists of

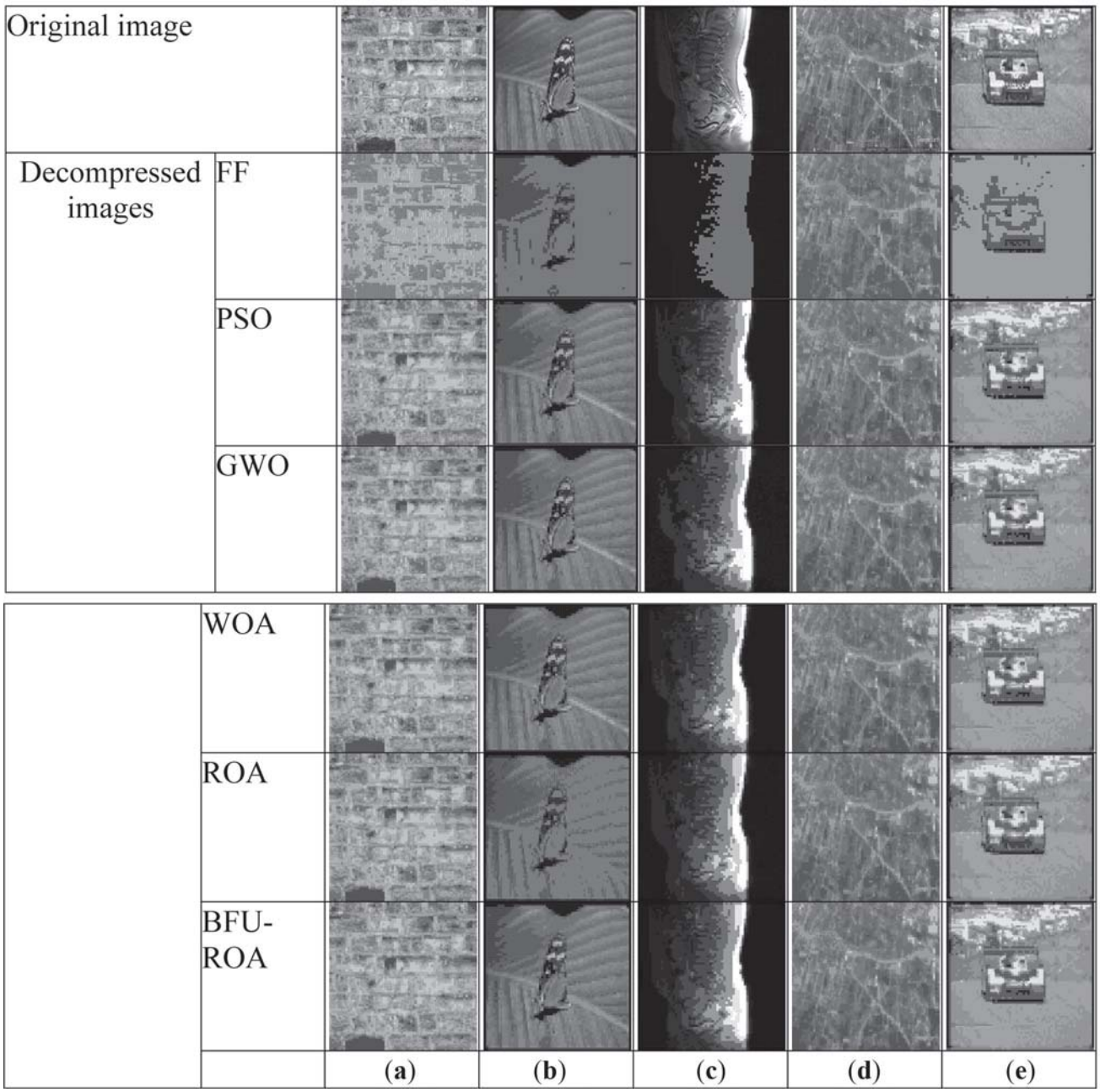

Figure 4. Sample images for original and decompressed images (a) Texture image, (b) Nature image, (c) Medical image, (d) Satellite image and (e) Miscellaneous image.

five data set including Texture image set (type 1 image), Nature image set (type 2 image), Medical image set (type 3 image), Satellite image set (type 4 image), and Miscellaneous image set (type 5 image). The texture images were downloaded from "(http://www-cvr.ai.uiuc.edu/ponce_grp/data/: access data 2019-06-11)", medical images were downloaded from "(http://www.ultrasoundcases.info/case-list.aspx?cat=26: access date 2019-06-11)", satellite images were manually collected, natural images were downloaded from "(http://www-cvr.ai.uiuc.edu/ponce_grp/data/: access data 2019-06-11)", and miscellaneous images were downloaded from two links "(http://vismod.media.mit.edu/pub/VisTex/, https://sites.google.com/site/dctresearch/Home/content-based-image-retrieval: access data 2019-06-11)". The analysis was held to examine the compression ratio and error between the original and decompressed images. For the analysis purpose, the proposed BFU-ROA was compared with conventional schemes such as FF [36], PSO [37], GWO [38], WOA [39] and ROA [35] algorithms. The

Table 2. Parameter value of the proposed method and conventional methods.

PSO	GWO	WOA	Proposed Model
Number of iterations=100	Number of iterations=100	Number of iterations=100	Number of iterations=100
Number of particles=200	Population size=200	Number of whales=20	Number of gears=5
Cognitive factor=1.4	Random numbers =0,1	a=2 to 0	Q_g = 0 and 4
Social factor=1,4	-	Random numbers=[0,1]	r_g = 0 and 1
Inertia weight=0.9 ∼ 0.4	-	-	a_g= 0 and 1
Random variables=[0,1]	-	-	β= 0 and 1
-	-	-	γ=1 and$X$
-	-	-	η= 1 and$X$
-	-	-	χ=0 and 1

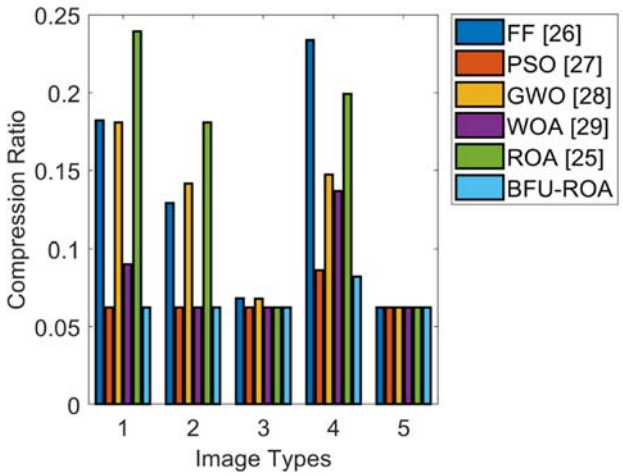

Figure 5. Compression ratio analysis of the Implemented and Classical models.

analysis was held for the proposed and conventional scheme regarding error measures such as SMAPE, RMSE, MEP, MAE, and MASE for five types of images. The sample images considered for image compression and the decompressed images based on proposed and conventional algorithms are shown in figure 4. Table 2 summarizes the parameter value of the proposed and conventional models.

5.2 *Analysis of compression ratio*

The analysis of compression ratio for the proposed BFU-ROA-based LBG is given by figure 5. From the analysis, for type 1 image, the presented BFU-ROA scheme is 61.11%, 61.11%, 22.22%, and 70.83% better than FF, GWO, WOA and ROA algorithms. Likewise, for type 2 images, the offered BFU-ROA method is 48.15%,50%, and 61.11% superior to FF, GWO, and ROA algorithms. In the same way, the proposed scheme for type 4 image is 60.87% improved than FF, 12.5% improved than PSO, 40% improved than GWO, 35.71% improved than WOA and 55% improved than ROA algorithms. Thereby the betterment of the implemented BFU-ROA method has been proved successful.

5.3 *Error analysis*

The error analysis of the proposed BFU-ROA approach for enhanced image compression is given in figure 4 with respect to varying weights. Eq. (8) shows the distance formula used for updating the bypass rider. For analysis purposes, the distance is multiplied with a weight function, as shown in Eq. (12).

$$Z_{g,h}^{\tau+1}(F) = Z^{L}(L, b) + \left[\cos\left(N_{g,b}^{\tau}\right) * Z^{L}(L, b) * \left(\eth_{g}^{\tau} * weight\right)\right] \tag{12}$$

In this analysis, the weight function is varied from 0.2, 0.4, 0.6, 0.8, and 1. From figure 6(a), at weight 1, type 1 image is 0.75% and 1.51% better than type 5 image and type 4 image. From figure 6(b), for SMAPE, at weight 1, the type 2 image is 8.06%, 7.56%, and 6.04% better than type 2 images, type 3 image and type 4 image. On considering figure 6(c), for MASE at weight 0.8, the type 5 image is 6.52%, 7.06% better than type 3 image and type 4 image. In addition, from figure 6(d), at weight 1, MAE for type 1 image is 5.74% and 3.25% better than type 2 image and type 4 image. Likewise, from figure 6(e), at weight 1, MAE for type 5 image is 4.29% and 3.1% better than type 2 image and type 4 image. From figure 6(g), at weight 1, MAE for type 5 image is 14.94% and 10.34% better than type 2 image and type 4 image.

The overall error analysis regarding image compression model that based on the proposed BFU-ROA is given in tables 3 to 7 for five types of images. From table 3, the presented scheme in terms of MEP is 2.65%, 2.69%, 2.71%, 2.69%, and 2.67% FF, PSO, GWO, WOA, and ROA algorithms. The adopted scheme in terms of SMAPE is 0.5% superior to all the compared algorithms. Likewise, the presented model in terms of RMSE is 1.01%, 0.99%,

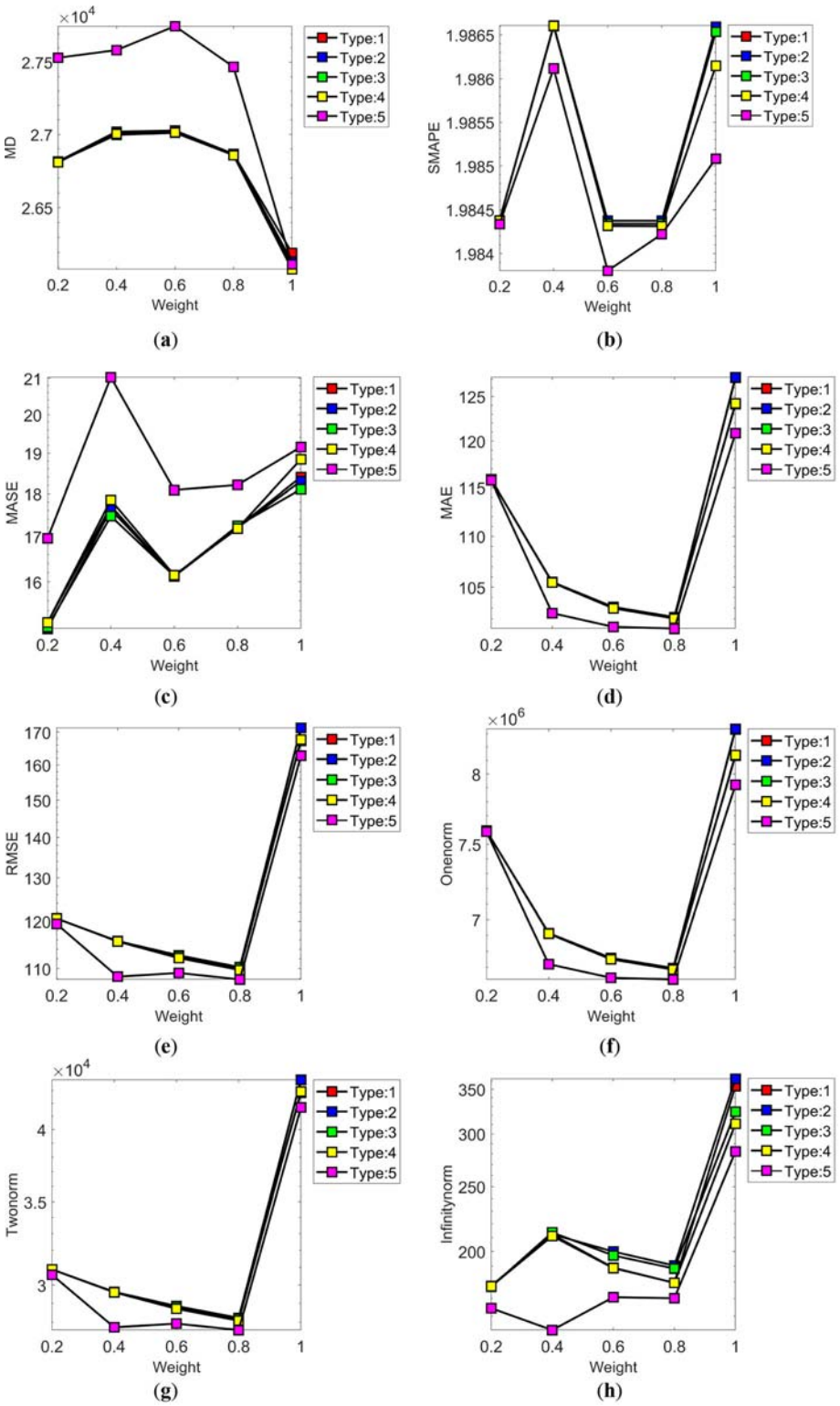

Figure 6. Error analysis of the Implemented and Classical models by varying weights (a) MEP, (b) SMAPE, (c) MASE, (d) MAE, (e) RMSE, (f) One norm, (g) Two norm and (h) Infinity norm.

0.98%, 0.99%, and 1.002% improved than FF, PSO, GWO, WOA, and ROA algorithms. Furthermore, from table 4, the implemented scheme for type 2 image with respect to MEP is 2.09%,2.13%, 2.18%, 2.15% and 2.14% improved than FF, PSO, GWO, WOA, and ROA algorithms. Similarly, the MASE of adopted scheme is 18.76%,19.34%, 20.39%,

Table 3. Error analysis of the Implemented and Classical approaches for type 1 image.

Methods	FF [36]	PSO [37]	GWO [38]	WOA [39]	ROA [35]	BFU-ROA
MEP	26821	26811	26805	26809	26817	27531
SMAPE	1.9844	1.9844	1.9844	1.9844	1.9844	1.9843
MASE	15.151	15.033	15.066	15.152	15.21	16.957
MAE	115.89	115.87	115.86	115.87	115.88	115.78
RMSE	120.66	120.64	120.63	120.64	120.65	119.44
One norm	7.59×10^6	7.59×10^6	7.59×10^6	7.59×10^6	7.59×10^6	7.59×10^6
Two norm	30888	30885	30880	30884	30887	30578
Infinity norm	177.49	177.25	177.06	177.28	177.55	164.39

Table 4. Error analysis of the Implemented and Classical approaches for type 2 image.

Methods	FF [36]	PSO [37]	GWO [38]	WOA [39]	ROA [35]	BFU-ROA
MEP	27019	27009	26996	27004	27007	27585
SMAPE	1.9866	1.9866	1.9866	1.9866	1.9866	1.9861
MASE	17.709	17.623	17.469	17.852	17.636	21.032
MAE	105.47	105.5	105.47	105.44	105.37	102.53
RMSE	115.7	115.73	115.73	115.64	115.56	108.37
One norm	6.91×10^6	6.91×10^6	6.91×10^6	6.91×10^6	6.91×10^6	6.72×10^6
Two norm	29620	29626	29627	29603	29585	27744
Infinity norm	212.14	212.25	213.59	210.98	209.12	152.42

Table 5. Error analysis of the Implemented and Classical approaches for type 3 image.

Methods	FF [36]	PSO [37]	GWO [38]	WOA [39]	ROA [35]	BFU-ROA
MEP	27027	27021	27011	27013	27030	27754
SMAPE	1.9843	1.9844	1.9843	1.9843	1.9844	1.9838
MASE	16.119	16.121	16.129	16.144	16.298	18.087
MAE	103	103.11	103.07	102.99	102.64	101.26
RMSE	112.17	112.72	112.57	112.16	111.74	109.12
One norm	6.75×10^6	6.76×10^6	6.75×10^6	6.75×10^6	6.73×10^6	6.64×10^6
Two norm	28716	28856	28818	28713	28605	27934
Infinity norm	189.06	199.94	197.28	188.85	198.68	170.71

Table 6. Error analysis of the Implemented and Classical approaches for type 4 image.

Methods	FF [36]	PSO [37]	GWO [38]	WOA [39]	ROA [35]	BFU-ROA
MEP	26866	26863	26858	26857	26869	27468
SMAPE	1.9843	1.9844	1.9843	1.9843	1.9844	1.9842
MASE	17.213	17.203	17.246	17.184	17.178	18.211
MAE	102.04	102.16	102.11	102.03	101.72	101.1
RMSE	109.73	110.29	110.13	109.72	109.34	107.82
One norm	6.69×10^6	6.70×10^6	6.69×10^6	6.69×10^6	6.67×10^6	6.63×10^6
Two norm	28090	28233	28194	28088	27991	27603
Infinity norm	179.42	190.48	188.53	179.47	189.26	170.16

Table 7. Error analysis of the Implemented and Classical approaches for type 5 image.

Methods	FF [36]	PSO [37]	GWO [38]	WOA [39]	ROA [35]	BFU-ROA
MEP	26197	26138	26119	26088	26724	26121
SMAPE	1.9866	1.9866	1.9865	1.9861	1.9858	1.9851
MASE	18.403	18.303	18.11	18.848	20.202	19.157
MAE	127.17	127.23	124.13	124.21	122.76	120.87
RMSE	171.3	171.36	167.25	167.64	167.16	162.77
One norm	8.33×10^6	8.34×10^6	8.13×10^6	8.14×10^6	8.05×10^6	7.92×10^6
Two norm	43853	43869	42817	42916	42793	41670
Infinity norm	353.94	363.04	323.78	310.73	300.55	282.26

Table 8. Statistical analysis of the Implemented and Classical approaches.

Methods	PSO [37]	FF [36]	WOA [39]	GWO [38]	ROA [35]	BFU-ROA
Best	0.0625	0.0625	0.0625	0.0625	0.0625	0.0625
Worst	0.23761	0.25907	0.33545	0.23371	0.23924	0.18079
Mean	0.14089	0.14265	0.13979	0.13513	0.14886	0.12004
Median	0.16697	0.16222	0.0625	0.12904	0.18084	0.14152
Std Deviation	0.076613	0.082729	0.11991	0.073689	0.081615	0.052268

Table 9. Computational time of the Implemented and Classical methods.

Methods	Computational Time (sec)
FF [36]	404.09
PSO [37]	377.51
GWO [38]	584.48
WOA [39]	327.29
ROA [35]	302.43
BFU-ROA	301.39

17.81%, and 19.26% improved than FF, PSO, GWO, WOA, and ROA algorithms. On considering type 3 image in table 5, the established structure in the view of MAE is 1.69%,1.79%, 1.76%, 1.68% and 1.34% improved than FF, PSO, GWO, WOA and ROA algorithms. Moreover, the RMSE of presented approach is 2.72%, 3.19%, 3.06%, 2.71%, and 2.34% enhanced than FF, PSO, GWO, WOA, and ROA algorithms. Similarly, on taking type 4 image from table 6, the two norm is 1.73% better from FF, 2.23% improved from PSO, 2.09% improved from GWO, 1.73% improved from WOA and 1.39% improved from ROA algorithms. Similarly, the infinity norm of adopted scheme is 5.16%,10.67%, 9.74%, 5.19%, and 10.09% enhanced than FF, PSO, GWO, WOA, and ROA algorithms. From table 7, the type 5 image for the adopted scheme can be attained, which is 4.98% better from FF, 5.01% better from PSO, 2.68% better from GWO, 2.9% better from WOA and 2.62% better from ROA algorithms in terms of RMSE. Thereby, the development of the established BFU-ROA approach is verified and proved by the simulated outcomes.

5.4 *Statistical analysis*

Table 8 summarizes the statistical analysis of the established and existing methods. Here, the established method is 36% improved than the FF method, 31% improved than the PSO, and 29% improved than the GWO, 56% better than the WOA, 35% better than the ROA algorithm for the standard deviation case scenario. Table 9 summarizes the computational time of the established and existing methods. Here, the established approach is 25% enhanced than the FF method, 20% enhanced than the PSO, and 48% enhanced than the GWO, 0.79% enhanced than the WOA, 0.034% better than the ROA algorithm.

5.5 *Result implication*

In this section, overall performance analysis of the proposed method over the conventional methods is shown. At first, the analysis of compression ratio for the proposed BFU-ROA-based LBG is performed. Here, the performance of the proposed method is 61.11%, 61.11%, 22.22%, and 70.83% enhanced than FF, GWO, WOA and ROA algorithms. Then, the proposed method in terms of SMAPE is performed. Here, the adopted approach is 0.5% better from all the compared algorithms. Similarly, the proposed method regarding RMSE is 1.01%, 0.99%, 0.98%, 0.99%, and 1.002% improved than FF, PSO, GWO, WOA, and

ROA algorithms. Moreover, the statistical analysis of the proposed is 36% better than the FF method, 31% enhanced than the PSO, and 29% better from the GWO, 56% better than the WOA, 35% better than the ROA algorithm. The overall analysis demonstrates that the established approach attains superiority over other existing models.

6. Conclusion

This work has exploited the VQ concept that makes use of the LBG model for image compression. Here, the database image was initially split into a set of blocks, and an appropriate codeword was chosen for every vector, which was the closest representation of that input vector. The encoder creates a codebook by mapping the vectors depending on these code words and accordingly, vector compression occurs. The encoder further transmits a compressed stream of these vectors to the decoder, which in turn discovers the compressed vector and places it on the image. As the main novelty, the code word creation in vector quantization was performed through a proposed optimization algorithm, so-called a BFU-ROA model for attaining an improved image compression effect. The optimization of codebooks was done, such that the summation of the compression ratio and the difference among the decompressed and original images should be minimal. From the analysis, for type 1 image, the established BFU-ROA structure was 61.11%, 61.11%, 22.22%, and 70.83% improved than FF, GWO, WO, and ROA algorithms. On taking the MEP, the presented approach was 2.65%, 2.69%, 2.71%, 2.69%, and 2.67% enhanced than FF, PSO, GWO, WOA, and ROA approaches. Thereby, the improvement of the BFU-ROA-based VQ for image compression was confirmed through perfect validation.

Nomenclature

ABC	Artificial bee colony
ACM	Active Contour Model
BER	Bit Error Rate
CFA	Color Filter Array
CMOS	Complementary Metal Oxide Semiconductor
CS	Cuckoo search
DCT	Discrete Cosine Transform
DTT	Discrete Tchebichef Transform
EZW	Embedded Zero-tree Wavelet
FIC	Fractal Image Compression
FSS	Fish School Search
GIF	Graphics Interchange Format
HV	Horizontal-Vertical
iDTT	integer DTT
JPEG	Joint Photographic Experts Group
LBG	Linde-Buzo-Gray
MAE	Mean Absolute Error
MASE	Mean Absolute Scaled Error
MEP	Mean Error Percentage
MF	Matrix Factorization
MSE	Mean Squared Error
OCR	Optimum Compression Ratio
PNG	Portable Network Graphics
PSNR	Peak Signal to Noise Ratio
QDCT	Quantum DCT algorithm
RMSE	Root Mean Square Error
ROI	Region Of Interest
ROI	Region of Interest
SERMs	Single-row Elementary Reversible Matrices
SMAPE	Symmetric Mean Absolute Percentage Error
SNR	Signal-to-Noise Ratio
VQ	Vector Quantization
WCE	Wireless Capsule Endoscopy

References

[1] Pang C-Y, Zhou R-G, Hu B-Q, Hu W W and El-Rafei A 2019 Signal and image compression using quantum discrete cosine transform. *Inform. Sci.* 473: 121–141

[2] Ernawan F, Kabir N and Zamli K Z 2017 An efficient image compression technique using Tchebichef bit allocation. *Optim. Int. J. Light Electr. Optim.* 148: 106–119

[3] Roy S K, Kumar S, Chanda B, Chaudhuri B B and Banerjee S 2018 Fractal image compression using upper bound on scaling parameter. *Chaos Solitons Fractals* 106: 16–22

[4] Brahimi T, Laouir F, Boubchir L and Ali-Chérif A 2017 An improved wavelet-based image coder for embedded grey-scale and colour image compression. *AEU Int. J. Electron. Commun*. 73: 183–192

[5] Xiao B, Lu G, Zhang Y, Li W and Wang G 2016 Lossless image compression based on integer discrete Tchebichef transform. *Neurocomputing* 214: 587–593

[6] Turcza P and Duplaga M 2017 Near-lossless energy-efficient image compression algorithm for wireless capsule endoscopy. *Biomed. Signal Process. Control* 38: 1–8

[7] Zuo Z, Lan X, Deng L, Yao S and Wang X 2015 An improved medical image compression technique with lossless region of interest. *Optim Int. J. Light Electron. Optim.* 126(21): 2825–2831

[8] Chaurasia V and Chaurasia V 2016 Statistical feature extraction based technique for fast fractal image compression. *J. Vis. Commun. Image Represent*. 41: 87–95

[9] Hussain A J, Al-Fayadh A and Radi N 2018 Image compression techniques: a survey in lossless and lossy algorithms. *Neurocomputing* 300: 44–69

[10] Mirjalili S and Lewis A 2016 The whale optimization algorithm. *Adv. Eng. Softw.* 95: 51–67

[11] Dimauro G, Caivano D and Girardi F 2018 A new method and a non-invasive device to estimate anemia based on digital images of the conjunctiva. *IEEE Access* 6: 46968–46975

[12] Fu C, Yi Y and Luo F 2018 Hyperspectral image compression based on simultaneous sparse representation and general-pixels. *Pattern Recognit. Lett.* 116: 65–71

[13] Gong L, Qiu K, Deng C and Zhou N 2019 An image compression and encryption algorithm based on chaotic system and compressive sensing. *Opt. Laser Technol.* 115: 257–267
[14] Ji X X and Zhang G 2017 An adaptive SAR image compression method. *Comput. Electr. Eng*. 62: 473–484
[15] Skorsetz M, Artal P and Bueno J M 2018 Improved multiphoton imaging in biological samples by using variable pulse compression and wavefront assessment. *Opt. Commun*. 422: 44–51
[16] Rashid F, Miri A and Woungang I 2016 Secure image deduplication through image compression. *J. Inf. Secur. Appl.* 27–28: 54–64
[17] Huang H, He X, Xiang Y, Wen W and Zhang Y 2018 A compression-diffusion-permutation strategy for securing image. *Signal Process*. 150: 183–190
[18] Balleyguier C, Cousin M, Dunant A, Attard M and Arfi-Rouche J 2018 Patient-assisted compression helps for image quality reduction dose and improves patient experience in mammography. *Eur. J. Cancer* 103: 137–142
[19] Liu H, Huang K-K, Ren C-X, Yu Y-F and Lai Z-R 2017 Quadtree coding with adaptive scanning order for space-borne image compression. *Signal. Proecess. Image Commun.* 55: 1–9
[20] Huang K-K, Liu H, Ren C-X, Yu Y-F and Lai Z-R 2017 Remote sensing image compression based on binary tree and optimized truncation. *Digit. Signal Process*. 64: 96–106
[21] Fister I, Fister I, Yang X-S and Brest J 2013 A comprehensive review of firefly algorithms. *Swarm Evol. Comput.* 13: 34–46
[22] Zhang J and Xia P 2017 An improved PSO algorithm for parameter identification of nonlinear dynamic hysteretic models. *J. Sound Vib.* 389: 153–167
[23] Mirjalili S, Mirjalili S M and Lewis A 2014 Grey wolf optimizer. *Adv. Eng. Softw*. 69: 46–61
[24] Gashnikov M V 2017 Minimizing the entropy of quantized post-interpolation residuals for hierarchical image compression. *Procedia Eng.* 201:196–205
[25] George A, Rajakumar B R and Suresh B S 2012 Markov random field based image restoration with aid of local and global features. *Int. J. Comput. Appl.* 488: 23–28. https://doi.org/10.5120/7369-0.137
[26] Vishwakarma B and Yerpude A 2014. A new method for noisy image segmentation using firefly algorithm. *Int. J. Sci. Res.* (IJSR) 3(5):1721–1725.
[27] Lalwani S, Sharma H, Verma A and Kumar R 2019 Efficient discrete firefly algorithm for Ctrie based caching of multiple sequence alignment on optimally scheduled parallel machines. *CAAI Trans. Intell. Technol.* 4(2): 92–100
[28] Karimi N, Samavi S, Soroushmehr S M R, Shirani S and Najarian K 2016 Toward practical guideline for design of image compression algorithms for biomedical applications. *Exp. Syst. Appl*. 56:360–367
[29] Kumar S N, Fred A L, Kumar H A, Varghese P S and Daniel A V 2017 *BAT Optimization-Based Vector Quantization Algorithm for Compression of CT Medical Images*. Springer, ICTIMI, Singapore.
[30] Fonseca C S, Ferreira F A B S and Madeiro F 2018 Vector quantization codebook design based on fish school search algorithm. *Appl. Soft Comput*. 73: 958–968
[31] Kumar B P S and K V Ramanaiah 2019 Region of interest-based adaptive segmentation for image compression using hybrid Jaya–Lion mathematical approach. *Int. J. Comput. Appl.* pp. 1–12
[32] El-Tokhy M S 2020 Ultimate neutron and x-ray radiography images compression using artificial bee colony and firefly optimization algorithms. *J. Electron. Imaging* 29(2): 023003
[33] Alturki A and Alrobaian A A 2019 A novel lossless image compression technique based on firefly optimization algorithm. *J. Eng. Appl. Sci.* 14: 2642–2647
[34] Binu D and Kariyappa B S 2019 RideNN: a new rider optimization algorithm-based neural network for fault diagnosis in analog circuits. *IEE Trans. Instrum. Meas*. 68(1): 2–26
[35] Saad A-M H Y and Abdullah M Z 2016 High-speed implementation of fractal image compression in low cost FPGA. *Microprocess. Microsyst.* 47 Part B: 429–440
[36] Li P and Lo K-T 2017 Joint image compression and encryption based on order-8 alternating transforms. *J. Vis. Commun. Image Represent*. 44: 61–71
[37] Zhou N, Zhang A, Wu J, Pei D and Yang Y 2014, Novel hybrid image compression–encryption algorithm based on compressive sensing *Optik Int. J. Light Electr. Opt.* 125(18): 5075–5080
[38] Zhu S, Zeng B and Gabbouj M 2015 Adaptive sampling for compressed sensing based image compression. *J. Vis. Commun. Image Represent.* 30: 94–105
[39] Chiranjeevi K and Jena U R 2018 Image compression based on vector quantization using cuckoo search optimization technique. *Ain Shams Eng. J.* 9: 1417–1431